Sheffield Hallam University

Sticky rice - nanolime as a consolidation treatment for lime mortars

STARINIERI, Vincenzo <http://orcid.org/0000-0002-7556-0702>, OTERO, Jorge and CHAROLA, Elena

Available from Sheffield Hallam University Research Archive (SHURA) at:

http://shura.shu.ac.uk/24411/

This document is the author deposited version. You are advised to consult the publisher's version if you wish to cite from it.

Published version

STARINIERI, Vincenzo, OTERO, Jorge and CHAROLA, Elena (2019). Sticky rice - nanolime as a consolidation treatment for lime mortars. Journal of Materials Science.

Copyright and re-use policy

See http://shura.shu.ac.uk/information.html

Sheffield Hallam University Research Archive
http://shura.shu.ac.uk

J Mater Sci

Composites

Sticky rice–nanolime as a consolidation treatment for lime mortars

J. Otero[1,2,*], A. E. Charola[3], and V. Starinieri[1]

[1] *Materials and Engineering Research Institute, Sheffield Hallam University, Sheffield S1 1WB, UK*
[2] *Getty Conservation Institute, The J. Paul Getty Trust, Los Angeles, CA 90049, USA*
[3] *Museum Conservation Institute, Smithsonian Institution, Washington, DC, USA*

Received: 14 February 2019
Accepted: 9 April 2019

© The Author(s) 2019

ABSTRACT

For almost 1500 years, many ancient Chinese mortars have remained unaltered despite exposure to atmospheric agents. The main reason for this long-term durability is the addition of sticky rice water to the standard mortar ingredients (lime and sand) following traditional recipes. In recent years, these mortars have been methodically studied leading to the conclusion that amylopectin, a polysaccharide in the sticky rice, plays a crucial role in regulating calcite crystals growth, creating a denser microstructure and providing the mortar with hydrophobic properties which contributed to their survival. In recent decades, nanolime products based on $Ca(OH)_2$ nanoparticles suspended in alcohol or hydro-alcoholic medium have been extensively used for the consolidation of calcareous substrates mainly due to their chemical affinity and absence of side effects. Nanolime products have resulted in successful superficial consolidations. However, in-depth consolidation still needs to be achieved, and research needs to focus on ways to attain this objective. This study aimed to test a novel approach consisting of applying a pre-treatment of sticky rice and subsequently the nanolime. The resulting consolidation was evaluated by measuring changes of superficial cohesion, porosity, contact angle, drilling resistance, water absorption by capillarity, drying rate and aesthetic properties. The durability of the treatments was investigated by exposing samples to accelerated weathering. Results showed that the use of sticky rice in combination with nanolime yields a higher degree of consolidation increasing drilling resistance and delivering hydrophobic properties although prolonged exposure to high temperature and moisture can compromise treatment durability.

Address correspondence to E-mail: Jotero@getty.edu; jorge.otero.h@gmail.com

https://doi.org/10.1007/s10853-019-03618-1

Published online: 17 April 2019

Springer

Introduction

Lime mortars have been used since historic times and to improve their texture and durability organic additives were included [1]. For example, oil from various sources, i.e., olive, linseed, or tallow, to make them water-repellent especially for limewashes; casein or blood as plasticizers; sugar, as setting retardants; egg white [2] to improve workability, and hair to increase their mechanical resistance. The selection of additives depended on the availability of the product, so olive oil was used in Mediterranean countries, such as Portugal and Italy, sugar in Brazil, and tallow in countries where sheep or cattle were abundant. Thus, each region developed its own specific tradition; in China, sticky rice was the preferred additive, this being the water in which sticky rice was cooked [3]. Rice contains two types of starch, amylopectin that makes rice sticky, and amylose that does not gelatinize; approximately 70% w/w of the starch is amylopectin, while amylose is only 5% w/w, and protein is also found, between 6.8 and 9.6% w/w, that could apparently influence the carbonation of the lime [4]. Amylopectin is a branched-chain polysaccharide composed of glucose units linked primarily by $\alpha-1,4$-glycosidic bonds but with occasional $\alpha-1,6$-glycosidic bonds, while amylose is a linear polysaccharide composed entirely of D-glucose units joined by the $\alpha-1,4$-glycosidic linkages [5, 6].

The sticky rice mortars were used in many historical buildings completed during the Ming (1368–1644) and the Qing (1644–1911) dynasties, such as the dyke at the Hangzhou Bay where the Quiantan river drains or the Jingzhou Historic Town Wall, one of the best preserved and largest historic town walls in Southern China that survived to date, [3, 7–11]. The earliest record of sticky rice–lime mortar was found in the ancient building book *Tian Gong Kai Wu* which was written during the Ming Dynasty (1368–1644 AD) [12]. However, there are archaeological evidence that show that they were also used during the South-North Dynasty (386–589 AD) [13]. According to ancient Chinese manuscripts, lime mortars used in those structures also contained sticky rice, although the formula for preparing the latter was not clear [14]. Although the sticky rice/lime mortar technology was well-known, these mortars had never been scientifically analyzed to understand the reasons for their good performance until the last decade. In 2008, several samples were prepared according to historic records of Chinese ancient books to determine the sticky rice/lime proportions and compared to samples taken from historic structures [3]. In this study, it was concluded that the microstructure of the prepared samples was very similar to that of ancient mortar samples, especially those containing a 3% volume ratio of sticky rice solution. This preliminary study also suggested that that sticky rice could play a crucial role in the microstructure and resistance of lime mortar as it functions as a template controlling the growth of calcium carbonate crystals. In subsequent years, many studies followed addressing the sticky rice/lime proportions [4, 8, 15, 16] and focusing on both the setting mechanism and the effect it had on improving the mechanical resistance [4, 7, 8, 15–18]. A systematic study of sticky rice–lime mortar technology was carried out varying sticky rice and lime content [15]. The physical properties, such as mechanical strength, were found to be significantly improved, especially those with 3% sticky rice solution. The authors also confirm that amylopectin, the main component of the sticky rice, acted as an inhibitor controlling the crystal growth of calcium carbonate creating a denser microstructure with smaller calcium carbonate crystals, explaining the good performance of these mortars. Other researchers found that the optimal sticky rice proportion when added to the lime mortar could vary from 1 to 3% [4] to 5% of sticky rice [7]. Further studies also showed that the formation of a more compact microstructure of smaller sized calcium carbonate crystals increases the mechanical properties, as calcium carbonate crystals are covered with a layer of sticky rice thus improving their resistance to weathering processes [4, 9, 10, 17–19]. The covering of the calcite crystals by the sticky rice in the mortar was also found to reduce the penetration of water in the structure and increase its resistance to wet–dry cycles [8, 18]. Additionally, this feature contributed to the higher seismic resistance of the mortars, as illustrated by the many ancient stupas, temples and bridges in Quan County built with sticky rice–lime mortar which survived the 7.5 earthquake of 1604 A.D [20].

Most of these studies differ in how the sticky lime mortars were reproduced, as they varied significantly from the traditional approach where sticky rice solution was added to the quicklime during quenching: "Usually, lime reacts with water to

generate hydrated lime with emission of a lot of heat and simultaneously create alkaline environment that can effectively suppress and kill bacteria" [7, 10] thus explaining why sticky rice did not undergo biodeterioration over time. Most studies use commercial hydrated lime [4, 8, 16], or slaked lime [15], while others prepared the "lime" solution by reacting a calcium chloride ($CaCl_2$) solution with Na(OH) [19] and in some cases using a supersaturated solution of this mixture and artificially carbonating it [3]. Nonetheless, most of the papers agree that the addition of sticky rice solution contributes significantly to the increase of the mortar's setting, mechanical strength, bonding capability, and reduced water absorption, though the study by Zhao et al. [16], which also addressed the addition of tung oil and pig blood, found that 5% sticky rice slurry "accelerates setting and hardening and increases compressive strength and bonding capability, although unit weight and water resistance are slightly reduced."

The fairly recent development of nanotechnology has brought new nanomaterials with potential superior properties. Nanolimes (dispersions of $Ca(OH)_2$ nanoparticles in alcohol or hydro-alcohol medium), were developed in the last decades as an effective and compatible conservation material for historic calcareous materials. Due to its high reactivity and compatibility, nanolimes resulted in successful superficial consolidation of historic substrates such as wall-paintings [21–23]. However, when an in-depth consolidation is required, their effectiveness is controversial since rarely do nanolimes attain penetrations above 1 cm [24]. Some studies focused on different ways to improve the nanolime in-depth consolidation effectiveness, for example, Daniele et al. [25] achieved faster and deeper consolidation by adding sodium bicarbonate ($NaHCO_3$) to the nanolime alcohol solution. However, the addition of $NaHCO_3$ may induce the formation of salt efflorescence. Furthermore, other studies focused on creating a CO_2-rich atmosphere in a yeast–sugar environment to accelerate the carbonation process and to increase the in-depth carbonation [26]. Recently, other studies suggested that the type of solvent could be critical for the nanolime effectiveness in highly porous substrates [27–29]. These studies suggest that solvents with low evaporation rate could be more suitable for coarse porous substrates as they would reduce the back-migration of the nanoparticles thus contributing to their in-depth deposition. However, more research needs to be carried out to elucidate the correlation between solvent, pore size distribution and penetration depth. From the current literature, it is clear that the consolidation effect of nanolimes still requires further study and more research needs to be carried out to study new ways to increase the nanolime in-depth consolidation effectiveness.

The present study focused on the effect sticky rice had when used as a pre-treatment before applying nanolime for consolidation of lime mortars. Physical properties, mechanical strength, penetration depth, water absorption, hydrophobicity and durability of samples treated by the combined treatment is compared with that of samples exposed to single treatments of either nanolime or sticky rice. This is an innovative approach and the results obtained are promising but several issues have as yet to be elucidated.

Materials and methods

Lime mortar samples

Lime mortars were prepared using a dry singleton Birch Ultralime CL90 and fine crushed silica sand ($0.07 < Ø < 1.5$ mm, Pentney, UK) in a binder/aggregate ratio of 1:2.5. Mortars were batched by weight after measuring the component densities in accordance with EN 1015-2:1998 [30]. The water/binder ratio was 1.56 to obtain a constant flow of 16 cm measured according to BS EN 1015-3:1999 [31]. The mixing and casting procedure of the mortar can be found elsewhere [24]. Mortar beams ($40 \times 40 \times 160$ mm) were de-molded after 5 days and then stored in an outdoor sheltered area ($T \approx 5$–15 °C, R.H $\approx$ 60–80%) for 28 curing days. Upon completion of the curing time, each prism was cut into approximately 4 cubes of $40 \times 40 \times 40$ mm prior to curing for another 28 days in the same conditions.

The mineralogical composition of the mortar was obtained by X-ray diffraction (PANalytical XPert PRO) recorded with a $0.02\mathring{6}2\theta$ step size in the angular range 20–70°2θ. X-ray data were refined by means of Rietveld refinement [32, 33]. The experimental diffraction pattern was elaborated by means of a Profile Fit Software (HighScorePlus, PANalytical), and each crystalline phase was identified using the ICSD and ICDD reference databases. The XRD

samples were ground and sieved through an 80 μm sieve mesh and placed over an XRD zero-background sample holder. The XRD-Rietveld refinements show the mortar to be composed of 79.9% Quartz (SiO_2, ICSD #00-046-1045) and 20.1% calcite ($CaCO_3$, ICSD #00-005-0586).

The pore structure of the mortar was determined by Mercury Intrusion Porosimetry (MIP) using a *PASCAL 140/240* instrument. The samples for MIP were mortar fragments measuring approximately 8 × 15 mm taken from the surface (up to a depth of 50 mm) of the sample, which were dried in an oven at 60 °C to constant weight. The average porosity of the mortar measured by MIP was 23 ± 1.6 vol% with a bulk density of 1.698 ± 0.1 g/cm^3.

Nanolime

Nanolime was synthesized through an anionic exchange process carried out at room temperature and ambient pressure by mixing under moderate stirring an anion exchange resin (Dowex Monosphere 550A OH by Dow Chemical) with an aqueous calcium chloride solution ($CaCl_2$ by Sigma-Aldrich), as described in the literature [34, 35]. After the synthesis, the newly synthetized nanoparticles of $Ca(OH)_2$ were dispersed in a 50–50% isopropanol/water solvent maintaining the concentration at 5 g/L, as this was found to be the optimal alcohol/water ratio [24, 35]. A description of morphology, reactivity and colloidal stability of this nanolime can be found in the latter reference.

Sticky rice

Commercial pulverized sticky rice was used in this study (Indica type, Enuo 6 variety) and was purchased from Erawan Marketing Co. TLD as "Farine de Riz Gluant" (product of Thailand). A well-known approach was followed to prepare the sticky rice starch suspension [4, 15, 36]. First, 2 g of pulverized sticky rice are added to 400 mL of deionized water (5 wt%) and left to soak for an hour. The suspension was then gradually heated (up to 300 °C) and stirred for 4 h. Afterward, the resulting paste was left to cool to $T \sim 30$ °C under vigorous stirring for approximately 1 h. The suspension was applied immediately after preparation.

Characterization of sticky rice

The compositions of the sticky rice powder and the prepared sticky rice paste suspension were studied by ATR-FTIR (Thermo Nicolet Nexus instrument). The dry sticky rice powder was ground (Ø < 150 μm), dried to constant mass at 60 °C and placed directly on the diamond crystal of the ATR accessory. For the sticky rice paste, a drop of the suspension was placed directly on the diamond crystal of the ATR accessory. FTIR spectra were collected by 64 scans in the range 400–4000 cm^{-1} at a spectral resolution of 4 cm^{-1}. A piece of aluminum foil was used to back the sapphire anvil to eliminate any sapphire absorption in the IR spectrum. The obtained FTIR spectrum was identified using the IRUG (Infrared and Raman Users Group) libraries [37], the HR Hummel Polymer and Additives library as well as the ASTER mineral library.

To further study the composition of the sticky rice, a starch–iodine test was conducted. The iodine reagent (KI) was prepared by dissolving 0.2 g of iodine in 100 mL of deionized water in the presence of 2.0 g of KI. Drops of the iodine-KI reagent were introduced into the sticky rice suspension. Sticky rice starch is a mixture of two types of polysaccharides: amylose and amylopectin [5]. The suspension turns blue in the presence of amylose or red in the presence of amylopectin [38].

The morphology of the sticky rice paste was observed by SEM (NOVA NANOSEM 200 instrument). SEM samples were prepared by placing a few drops (± 0.10 mL) of sticky rice suspension on a carbon film on a copper SEM sample holder. SEM micrographs were taken with an ETD detector, a working distance of ≈ 3 mm, an accelerating voltage of ≈ 15 kV and a spot size of ≈ 30 nm in high vacuum (25 MPa). Specimens were coated with a 20 nm thick layer of gold using a Quorum Q150T coater unit at 10 MA sputter current and 420 s sputter time.

The rheological behavior of the sticky rice suspension was measured using a Rheometer (Anton-Paar Physica MCR 301), since viscosity is an important factor for the penetration of a liquid in a porous material [39]. The measurements were made at 30 °C. The obtained flow curves plot the shear stress (mPa) versus the velocity gradient (s^{-1}) and were compared to that of water.

The surface tension of the sticky rice suspension was determined by the pendant drop method using

an OCA 15 Plus instrument (Dataphysics). For this test, a sticky rice suspension drop (5 μL) was pendant through a Hamilton 50 μL DS 500/GT syringe. The surface tension of the sticky rice was calculated by measuring the shape of the pendant drop of the dosing needle, defined with the Young–Laplace equation:

$$\Delta P = \gamma\left(\frac{1}{R1}+\frac{1}{R2}\right)$$

where "ΔP" is the difference in pressure across the interface, "γ" the surface tension, and "$R1$" and "$R2$" are the curvature radius.

Sticky rice and nanolime application

The sticky rice and nanolime were applied on three 40 × 40 × 40 mm lime–mortar cubes following the application method described below. Three cubic mortars were treated with nanolime (LAQ), three with sticky rice (SR) and three with a combination of sticky rice and nanolime (SR-LAQ).

The sticky rice suspension was used both as a consolidant and a pre-treatment prior to the nanolime application. As a consolidation treatment, the sticky rice suspension was applied by brush in laboratory conditions (∼ 50%RH) on only one face of the specimen until no further absorption was observed for a period of at least 5 min between each brushstroke. The sticky rice was absorbed throughout the cubic samples reaching the opposite face. Upon completion the treatment, the samples were dried in an oven to accelerate water evaporation at 30–40 °C to constant mass. Samples were weighed before and after application, once constant weight was reached, to determine the total amount of the absorbed dry sticky rice product by each substrate.

As a pre-treatment, the sticky rice solution was applied following the above description and once the samples reached constant mass, the nanolime was immediately brushed on the same face of the specimen. The nanolime dispersion was applied 2 days after its synthesis to increase its effectiveness [40]. The nanolime dispersion was agitated before application to increase the colloidal stability of the particles [24]. The application was ended when no further absorption was observed (surface remains completely wet for a period of at least 1 min). The nanolime was also absorbed throughout the cubic samples reaching the opposite face. Samples were also weighed after application to determine the total amount of nanolime absorbed by each substrate.

A complete description of the application method of nanolime can be found elsewhere [24]. Upon treatment completion, the treated samples were stored for 28 days at outdoor environment conditions (70 ± 5% RH, T = 10 ± 5 °C). A set of untreated control samples was stored under the same outdoor conditions, and are referred to as CO.

Consolidation effectiveness

Following the 28-day outdoor exposure, the treated and untreated lime mortar cubes were dried to constant mass at 60 °C in a fan-assisted oven and subsequently stored in a desiccator until testing.

Pore size distribution and porosity were measured by MIP (Pascal Inst.140/240). Tests were carried out on two samples taken from the surface (up to a depth of 50 mm) of treated and control mortars. Contact angle of the mercury and treated samples was taken to be 140°. Samples were dried to constant mass at 60 °C for 24 h prior to the analysis.

Water absorption coefficient (WAC) and capillary absorption curves were obtained [41]. Upon completion of this test, the samples were immersed in water for 24 h and then weighed at room conditions to calculate the apparent and open porosity [42]. Finally, the drying behavior was also determined [43]. This test sequence was carried out on three control specimens and three treated specimens per each treatment.

Surface cohesion of the specimens after treatment was evaluated by the "Scotch Tape Test" (STT) according to ASTM D3359 [44]. The test was performed on both treated and control samples, and results were taken as the average of 9 measurements per sample.

The penetration and consolidation effectiveness of the treatments was also assessed by means of a Drilling Resistance Measurement System (DRMS) from SINT-Technology [45, 46]. Tests were performed on both control and treated samples using drill bits of 5 mm diameter, a rotation speed of 600 rpm, a penetration rate of 15 mm/min and a penetration depth of 20 mm. Drilling resistance values were calculated as the mean of 6 tests carried out on 2 specimens per each treatment.

The hydrophobic behavior of the treatments was determined by contact angle measurements (OCA 15

Plus, Dataphysics Instrument), to determine the wettability of the substrates after the applied treatments. For this test, a water drop (5 μL, deionised water) was placed over the substrate surface using a Hamilton 50 μL DS 500/GT syringe. Pictures of the water drop on specimens´ surfaces were taken 1 s after applying the water drop and the contact angle was calculated by the software. The static contact angle (θ) reported was the average of 10 measurements.

Changes in color were determined by means of a spectrophotometer (Minolta CM508D Colorimeter) with the CIE-Lab system [47], using 30 readings taken in different areas of the surface of each of the treated and control samples. Total color variation (ΔE) was calculated by the formula:

$$\Delta E = \sqrt{\Delta L^{*2} + \Delta a^{*2} + \Delta b^{*2}}$$

where ΔL^*, Δa^* and Δb^* are the change in luminosity for white–black, red–green and blue–yellow parameters, respectively.

Durability of the consolidation treatments

The durability of the sticky rice and sticky rice–nanolime treatments was assessed by exposing three mortar samples treated with SR and three treated with SR-LAQ to Accelerated Weathering (AWT, QUV/SE Accelerated Weathering Tester from Q-Lab Europe Ltd) under two different exposure conditions:

- AWT 1: Step 1: 8 h UV at 1.55 W/m^2 irradiance and 60 °C; Step 2: 4 h moisture condensation at 50 °C with no UV irradiation (ASTM G154 CYCLE 6). Duration 340 h.
- AWT 2: Step 1: 8 h UV at 1.55 W/m^2 irradiance and 40 °C; Step 2: 4 h moisture condensation at 30 °C with no UV irradiation. Duration 340 h.

To further assess the durability of the treatments, the resistance to wet–dry cycles was evaluated following a method described in the literature [8]. Three cubic specimens for both SR and SR-LAQ were used for this test. During the experiment, all the samples were immersed in deionized water for 8 h, with the water level 20 mm over the samples' upper surface. After thoroughly soaked, the samples were put into the fan-assisted oven (40 °C) for 8 h, and then naturally cooled to the normal atmospheric temperature. This cycle was repeated 20 times.

After both the weathering in the QUV and the wet–dry test, the durability of the treated samples was assessed by measuring changes in the mortar's superficial cohesion (by Scotch Tape Test), drilling resistance (DRMS) and hydrophobic properties (contact angle). A small amount of water used from the wetting–drying cycles were also analyzed by FTIR to study its composition after the last cycle.

Results

Characterization of the sticky rice solution

The dried sticky rice paste was first examined by SEM immediately after water evaporation (Fig. 1). The dried gelatinized sticky rice presents an uneven structure formed by a film with several granular nodules tightly packed and clustered into compound grains surrounded by some protein which may

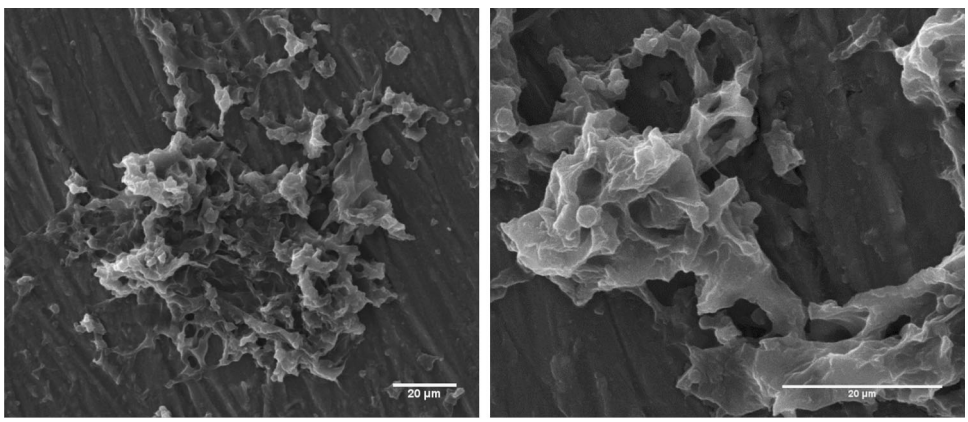

(a) (b)

Figure 1 SEM images of the sticky rice. **a** 2000×; **b** 5000×.

influence the carbonation rate of lime putty, similar as observed in the literature [4] (Fig. 1).

ATR-FTIR analysis of the dried sticky rice paste showed absorbance bands that can be attributed to rice starch (IRUG-ICB00021). The absorbance band at 847 and 761 cm^{-1} is attributed to the C-O group from the glucose anhydride ring, and the absorption bands at 3271 and 1654 cm^{-1} can be attributed to the absorbance of the –OH groups in the starch [15, 48]. According to the latter reference this rice starch spectrum can be attributed to amylopectin (supplementary Information).

A red–brown color was very evident after the addition of the iodine–KI reagent to the sticky rice solution [38] which clearly indicates that the sticky rice starch used was mainly composed of amylopectin (supplementary information).

Rheological analysis shows that the sticky rice suspension presents a constant complex viscosity between 0.002 and 0.001 mPa s, similar to water (supplementary information), and significantly lower viscosity than that of other consolidation products used in cultural heritage such as PEG (poly(ethylene glycol)) [49].

The surface tension of sticky rice was 69.28 (± 0.81) mN/m and very similar to that of water (69.99 (± 0.5) mN/m) (Fig. 2).

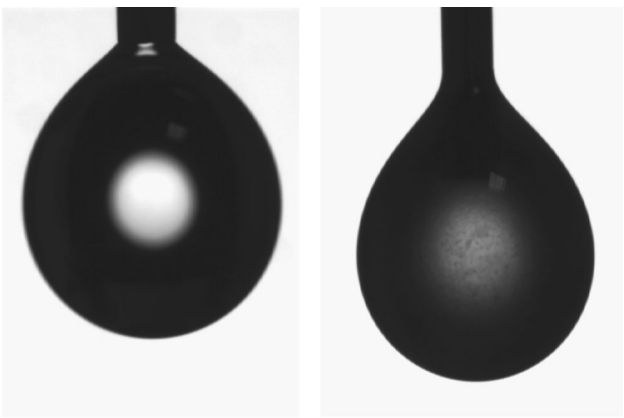

(a) (b)

Figure 2 Analysis of the pendant surface angle of: **a** water (69.99 mN/M); **b** sticky rice solution (69.28 mN/m).

Consolidation effectiveness

The apparent and open porosity of treated and control samples was calculated after 24 h of total immersion in water, and the actual pore size distribution was measured by MIP (Table 1). It can be seen that all treatments slightly reduced both apparent and open porosity of the mortar, although the high standard deviation, particularly for the LAQ samples, makes this decrease not statistically significant. The porosity reduction was confirmed by the MIP data; the highest decrease in porosity corresponds to the samples treated with sticky rice and nanolime, SR-LAQ (~ 22.9% decrease), followed by those treated with nanolime only, LAQ, and sticky rice only, SR (13.14% and 12.8%, respectively). This can be attributed to the higher amount of consolidant product remaining in the samples (SR-LAQ) after solvent evaporation, corresponding to 0.605 g (0.55 g of sticky rice and 0.055 g of LAQ), while for SR about 0.55 g remained whereas only 0.055 g remained of LAQ (both SR-LAQ and LAQ introduced the same amount of nanolime).

The pore size distributions of treated and control samples are shown in Fig. 3. The MIP curves clearly show that the reduction in porosity produced by all treatments can be attributed to a decrease in the number of pores with diameters between 2 and 11 μm. The nanolime only (LAQ) and sticky rice–nanolime (SR-LAQ) treatments also reduced the population of pores with diameters between 0.01 and 0.3 μm, the latter treatment yielding a slightly more marked decrease. LAQ treatment also slightly reduced the population of pores with diameters between 0.5 and 1 μm.

The water contact angle of treated samples was carried out to determine if any hydrophobic properties were induced to the mortar by the sticky rice and the sticky rice–nanolime treatments. The static contact angle (θ) on samples treated with LAQ is 0. Figure 4 shows the static contact angle (θ) on the surfaces treated with SR and SR-LAQ. In both cases, the application of sticky rice increases the

Table 1 Calculated Apparent porosity (% g/g) and open porosity (% cm^3/cm^3), and porosity by Hg intrusion (%)

	CO	LAQ	SR	SR-LAQ
Apparent porosity % w/w	12.22 (± 0.84)	12.16 (± 1.09)	12.05 (± 0.28)	11.73 (± 0.19)
Open porosity % v/v	17.26 (± 0.56)	17.01 (± 1.71)	16.82 (± 0.63)	16.88 (± 0.14)
Porosity by Hg intrusion (%)	18.8	16.33	16.44	14.46

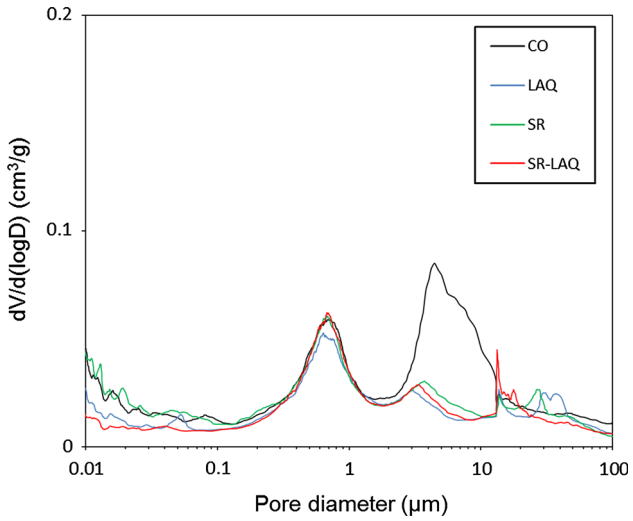

Figure 3 Differential volume of intruded mercury versus pore diameter of samples treated with LAQ, SR and SR-LAQ.

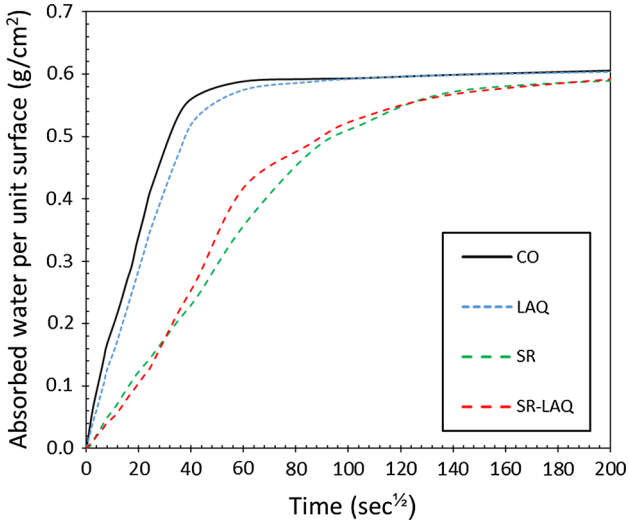

Figure 5 WAC curves of control and treated samples.

hydrophobicity of the treated surface. The static contact angle on SR samples is 106° (± 4.6), which confirms the surface hydrophobicity; while the static contact angle on SR-LAQ is 66° (± 5.41), suggesting that the hydrophobicity of the treated surface decreases when the application of sticky rice is followed by that of nanolime. The different hydrophobicity of the treated surfaces is likely to affect the contact angle between these and the mercury, which in this study was taken to be 140°. This has to be considered when interpreting the results of the MIP measurements shown in Fig. 4 and a detailed study is required in order to address this issue.

The capillary water absorption (WAC) of treated samples is shown in Fig. 5 where it can be seen that all treated samples show a reduced water absorption (Table 2). The highest decrease was observed for samples treated with sticky rice only (SR), followed by those treated with sticky rice and nanolime (SR-LAQ) and those treated with nanolime only (LAQ). Table 2 also shows that all treated samples absorb slightly less water when all capillaries are filled, although the high standard deviation makes the results not statistically significant.

Control and LAQ samples reached asymptotical absorption values after 20 min of contact with water, while samples treated with sticky rice only (SR) and sticky rice and nanolime (SR-LAQ) needed approximately 5 h (Fig. 5), which clearly confirms that the sticky rice reduces the speed of water absorption by capillarity.

The drying curves are shown in Fig. 6. All treated samples present slightly different initial drying rate (from 0 to 25 h) and similar final drying kinetics (from 35 to 50 h). LAQ presents slightly slower initial drying rate followed by SR and SR-LAQ (Table 2). All treated samples were completely dry after 50 h, similarly to control samples. This confirms that the application of sticky rice or nanolime does not interfere significantly with the water evaporation of the wet samples, which is desirable as this will

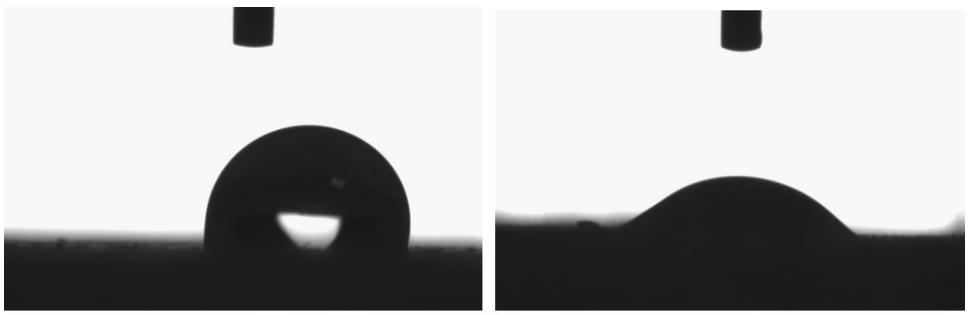

Figure 4 Static contact angle images after 1 s. **a** SR (106° ± 4.6); **b** SR-LAQ (66° ± 5.4).

Table 2 Water absorption and drying characteristics

Parameter	CO	LAQ	SR	SR-LAQ
W. absorption coefficient (10^{-3} g/cm^2 s$^{0.5}$)	19.1 (± 0.6)	15.1 (± 0.8)	7.0 (± 2.5)	10.1 (± 2.0)
W. absorbed at asymptotic value (g)	10.32 (± 0.70)	10.17 (± 0.92)	9.59 (± 0.80)	10.05 (± 0.10)
W. absorbed 24 h immersion (g)	10.32 (± 0.70)	10.17 (± 0.92)	9.59 (± 0.80)	10.05 (± 0.10)
Initial drying rate (10^{-3}g/cm^3 h)	9.7 (± 0.2)	9.5 (± 0.3)	7.7 (± 0.3)	7.5 (± 0.3)
Final drying rate (10^{-3}g/cm^3 h)	2.7 (± 0.3)	3.4 (± 0.2)	3.1 (± 0.4)	3.3 (± 0.4)
Time for total drying (h)	± 50	± 50	± 50	± 50

Values in parentheses are standard deviation calculated from the three samples. W (water)

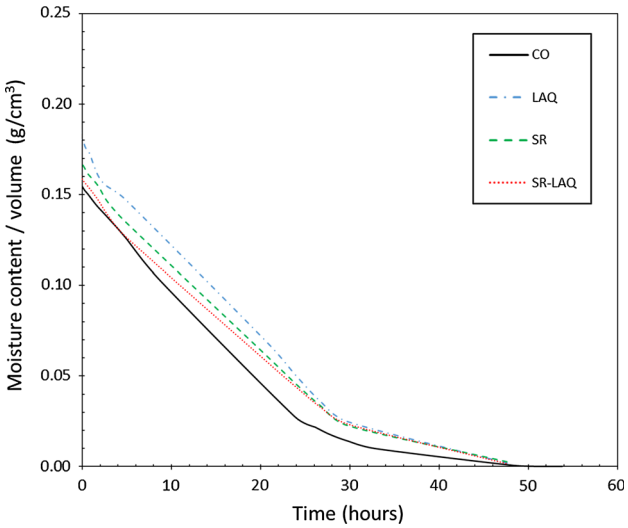

Figure 6 Drying curves of control and treated samples.

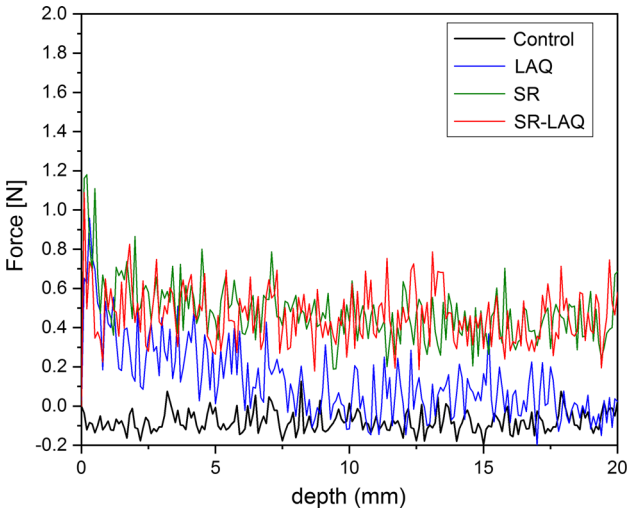

Figure 7 DRMS of treated and untreated samples.

reduce deterioration mechanisms such as biodeterioration or salt damage [50].

The results of the Scotch Tape Test (STT) are shown in Table 3. All treatments yielded decreasing values of removed material (21.9–5.77 mg/cm^2). These results confirm that all surfaces are more compact after treatment ($\Delta W \approx$ 74.1–96%). The samples treated only with sticky rice and those with sticky rice and nanolime showed a higher increase in surface cohesion ($\Delta W \approx$ 96% and $\Delta W \approx$ 93%, respectively) than those treated by nanolime only ($\Delta W \approx$ 74%).

Drilling resistance results for treated and untreated samples are shown in Fig. 7. The force required to drill a hole at constant rotation and lateral feed rate is known to correlate with the compressive strength of the material [46]. The samples treated with nanolime only (LAQ) show a slightly increased drilling resistance ($F \sim$ 0.13 (± 0.19) N, $\Delta F \sim$ 62%) within about 6–8 mm from the surface, which is in line with the results of previous research [24]. Drilling resistance of the samples treated with sticky rice (SR) and with sticky rice and nanolime (SR-LAQ) is higher than those of the control and of that treated only with nanolime, and they have a fairly constant value throughout the drilling depth (Fig. 7). It is important to note that during the application of the sticky rice, in both SR and SR-LAQ samples, the solution reached the opposite side of the cubic sample, indicating that it is likely that the internal porosity of the sample was

Table 3 Scotch Tape Test (STT): experimental results

	Released material (mg/cm^2)	ΔW (%)	SD
CO	84.59	–	12.01
LAQ	21.9	74.12	6.09
SR	3.04	96.41	3.5
SR-LAQ	5.77	93.18	5.6

Scotch area: 3 × 1.5 cm; SD (standard deviation of released material)

covered by a sticky rice film. DRMS patterns indicate that sticky rice provides a deeper consolidation of the mortar independent of the use of nanolime in combination with it. Since both LAQ and SR-LAQ samples received the same amount of nanolime particles, DRMS patterns also suggest that the nanolime introduced in the SR-LAQ samples could have been distributed more homogeneously throughout the pore structure rather than being accumulated in the outer 6–8 mm. Further research is required to elucidate these hypotheses.

SEM images show morphological differences between samples treated with sticky rice only and those treated with sticky rice and nanolime (Fig. 8). SR samples show that the sticky rice is homogeneously distributed as a film over the mortar grains (Fig. 8a, b). In contrast, SR-LAQ samples show that the calcite crystals of LAQ grow embedded in this film as they crystallize upon carbonation (Fig. 9c, d), as reported in the literature [4, 15]. However, the morphology and size of those calcite crystals were not reduced in size, as reported in studies of both ancient and recent Chinese lime–mortars with sticky rice [4, 9, 10, 17–19]. The calcite crystals were found to be similar to the ones observed in preliminary studies with the same nanolime [24].

Colorimetry results (Table 4) show that the treatments involving nanolime (LAQ and SR-LAQ) caused a whitening effect on the surface, with both ΔE^* and ΔL^* values above 5, especially for samples treated with only nanolime (LAQ). The increase in whitening is attributed to the accumulation of nanolime particles on the surface, as described in previous studies [24]. In contrast, SR samples do not show any aesthetic alterations.

Durability of the consolidation treatments: comparison between AWT-1 (@50 °C), AWT-2 (@30ª C) and wet–dry cycles

Scotch Tape Test

Results of the STT show that the surface cohesion obtained during the consolidation treatment, decreased significantly for SR and SR-LAQ samples in the case of the 50 °C weathering and somewhat

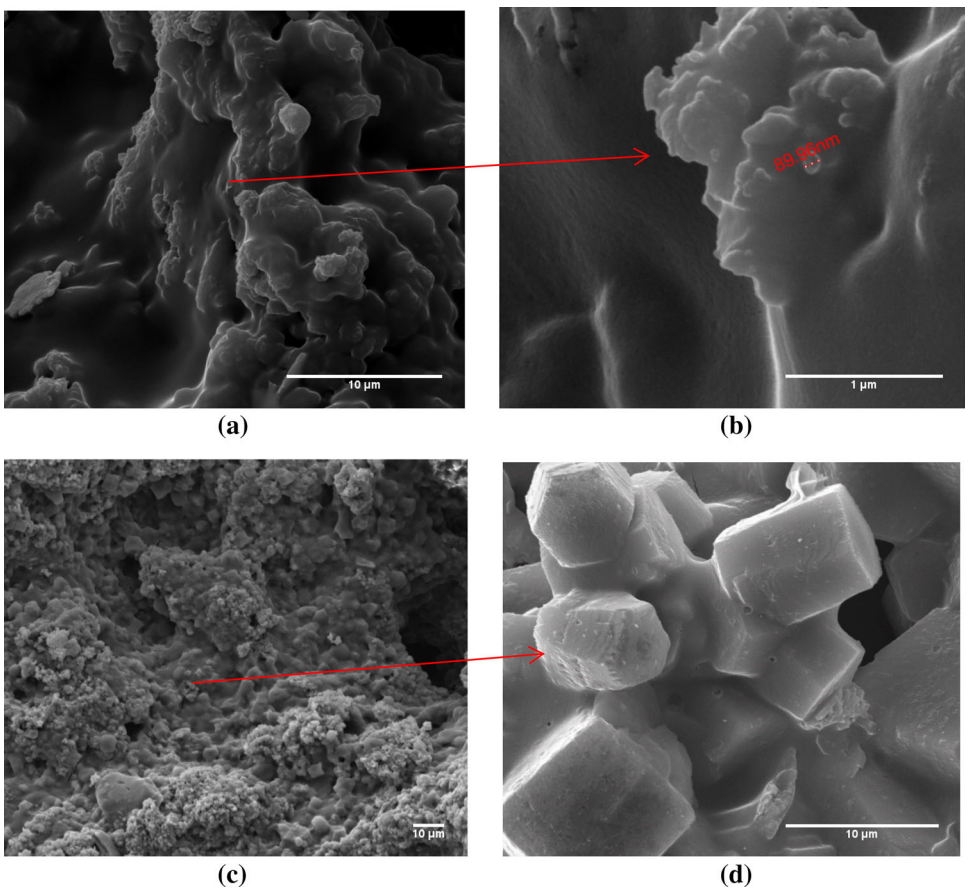

Figure 8 SEM images of **a** SR at 10,000×; **b** SR at 100,000×; **c** SR-LAQ at 2,000×; **d** SR-LAQ at 10,000×. Red arrow shows location of the magnified crystals in the sample.

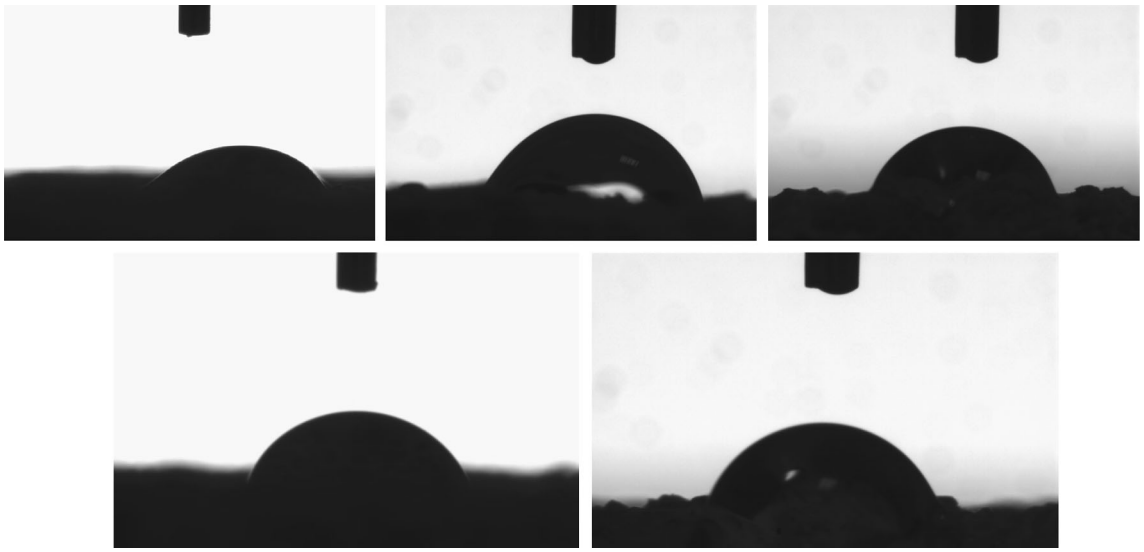

Figure 9 Static contact angle of treated samples after: Top line: Left sample treated with SR (20.6° ± 3.14) after AWT-1 (T = 50–60 °C); center sample treated with SR (80.2° ± 8.83) after AWT-2 (T = 40–30 °C); Right sample treated with SR-LAQ (69.26° ± 8.83) after AWT-2 (T = 40–30 °C); Bottom line: Samples after wet–dry cycling, Left, sample treated with SR (71.1° ± 6.12); Right, sample treated with SR-LAQ (42.8° ± 5.15).

Table 4 Chromatic alterations for treated samples

	ΔL^*	Δa^*	Δb^*	ΔE^*
LAQ	11.94 (± 0.97)	− 1.25 (± 0.26)	− 6.96 (± 1.04)	13.87
SR	2.19 (± 2.35)	− 0.56 (± 0.24)	− 1.20 (± 0.74)	2.55
SR-LAQ	7.99 (± 1.72)	− 0.59 (± 0.48)	− 1.91 (± 0.83)	8.23

Mean values determined 30 measurements

less for the 30 °C regime and wet–dry cycles (Table 5). The decrease is more pronounced for samples treated only with sticky rice. This can be explained by the fact that the applied nanolime treatment would protect somewhat the sticky rice film as seen in SEM. Control samples confirm that AWT cycles did not affect the surface cohesion of the mortar. Wet–dry cycling reduced even less the surface cohesion.

Water contact angle

The water contact angle measured on the samples after AWT-1 shows that the hydrophobicity of the samples treated with SR and SR-LAQ was significantly reduced (Fig. 9). The contact angle is 0° on the sample treated with SR-LAQ, and 20.6° (± 3.14) on the sample treated with SR (Fig. 9), clearly suggesting that the sticky rice, which was responsible for the hydrophobic effect was lost during this aging process. However, for the AWT-2 conditions, the water contact angles of samples treated with SR and SR-LAQ are 80.16° (± 3.18) and 69.26° (± 8.83), respectively, indicating that the sticky rice is still present on the sample surface. While the static contact angle clearly decreased in SR samples from approximately 106° to about 80° (before and after AWT-2) there was a minimum change for the SR-LAQ samples, from approximately 66° to about 69° (before and after AWT 2), suggesting that the nanolime treatment protected the sticky rice. After wet–dry cycling, the sample treated only with sticky rice retained an angle of about 71°, while that treated also with nanolime decreased to about a 43° angle.

Drilling resistance

For both samples, SR and SR-LAQ, drilling resistance significantly decreased after AWT-1 (50 °C), which is in line with the STT and the contact angle results described above. The drilling resistance of SR samples was reduced to values close to those of the

control sample (Fig. 10). In contrast, the drilling resistance of SR-LAQ remained similar to that recorded before the AWT-1 within about 2 mm from the surface and decreased to values slightly above those of the control throughout the remaining drilling depth. The more durable consolidation effect on the SR-LAQ samples compared to SR samples could be attributed to the effect of nanolime on this sample. In the case of the AWT-2 (30 °C), both samples also show a decrease in resistance, following the same pattern as for STT tests, suggesting that the starch also partially degrades under these conditions. In the case of wet–dry cycles, drilling profiles are similar to those observed for samples exposed to AWT-2 (at T = 30–40 °C) confirming that the degradation of starch can also occur at room conditions if sufficient water is available. In all cases, the decrease in the drilling resistance is significantly more pronounced in SR samples than in SR-LAQ samples, confirming the results obtained for the contact angle and STT. Wet–dry cycling showed a similar decrease in the two samples.

Results of STT, contact angle and DRMS clearly show that the consolidating effect of the sticky rice is lost during the AWT-1 cycling and can be attributed to the higher temperatures (T = 60–50 °C), which may have degraded the sticky rice starch due to the presence of water and heat, especially at temperatures above 55 °C where starch undergoes an irreversible gelatinization process [51], where the water dissolves starch granules by breaking down the intermolecular bonds of starch molecules [52]. This process turned the sample a yellowish color ($\Delta E \sim 3$). Therefore, for both samples (SR and SR-LAQ), the sticky rice is partially solubilized and washed out of the sample during the AWT-1 aging.

These results suggest that the degradation of sticky rice is higher when it is applied on its own rather than when applied in combination with nanolime treatment, where the calcite crystals grow up embedded in the sticky rice film (as shown in Fig. 8d). This might increase the adhesion to the mortar as both calcite and starch film may bond to the grains and matrix physically and chemically thus making the sticky rice slightly more resistant to solubilization. In contrast, when the sticky rice solution is applied without nanolime, it forms a film over the substrate grains (Fig. 8b), which may suggest that this film only adheres to the mortar grains physically, thus, more likely to solubilize as it does not bond chemically to the mortar.

Figure 10 DRMS of samples before and after weathering cycle: Top line: Left: SR after AWT-1 (T = 50–60 °C); Right: SR-LAQ after AWT-1 (T = 50–60 °C); Center line: Left: SR after AWT-2 (T = 30–40 °C); Right: SR-LAQ after AWT-2 (T = 30–40 °C); Bottom line: Left, SR after wet–dry cycles); Right: SR-LAQ after wet–dry cycles.

Fourier-transform infrared spectroscopy (FTIR)

To confirm the solubilization of the sticky rice, ATR-FTIR analysis was carried out on the water used for the wet–dry cycles. This analysis clearly shows that the water contains some small traces of sticky rice confirming the partial dissolution of some starch in the water. The absorbance band between 1000 and 1500 cm^{-1} is attributed to sticky rice (supplementary information).

Discussion

The present study aimed to address the effect that sticky rice (SR) had on mortar samples when applied as both a consolidant and pre-treatment before

Table 5 Results of the Scotch Tape Test (STT) after the weathering processes

	Released material (mg/cm^2) before weathering	ΔW (%) before weathering	Released material (mg/cm^2) after AWT1	ΔW (%) after AWT1	Released material (mg/cm^2) after AWT2	ΔW (%) after AWT2	Released material (mg/cm^2) after wet–dry	ΔW (%) after wet–dry
CO	84.59 (± 12.01)	–	83.12 (± 15.7)	–	83.32 (± 13.1)	–	82.98 (± 12.2)	–
SR	3.04 (± 3.5)	96.41	18.64 (± 3.21)	77.6	11.1 (± 1.4)	86.65	9.92 (± 0.98)	88.07
SR-LAQ	5.77 (± 5.6)	93.18	12.88 (± 1.08)	84.51	8.74 (± 0.88)	89.49	10.02 (± 1.45)	87.73

Scotch Tape Test area: 3 × 1.5 cm; in parenthesis are the standard deviations

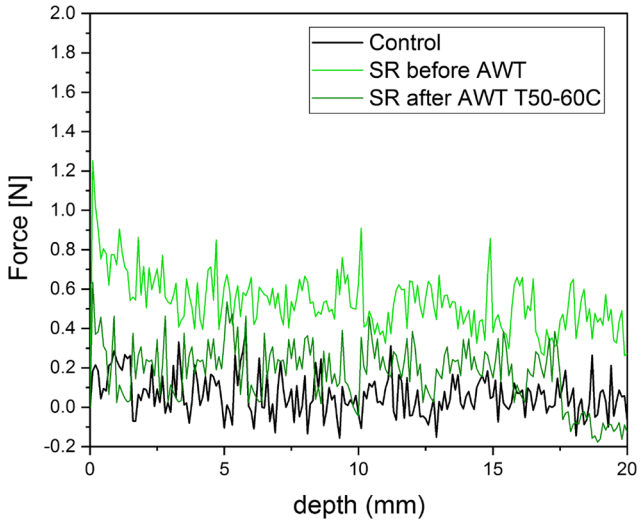
Control
SR before AWT
SR after AWT T50-60C
Force [N]
depth (mm)

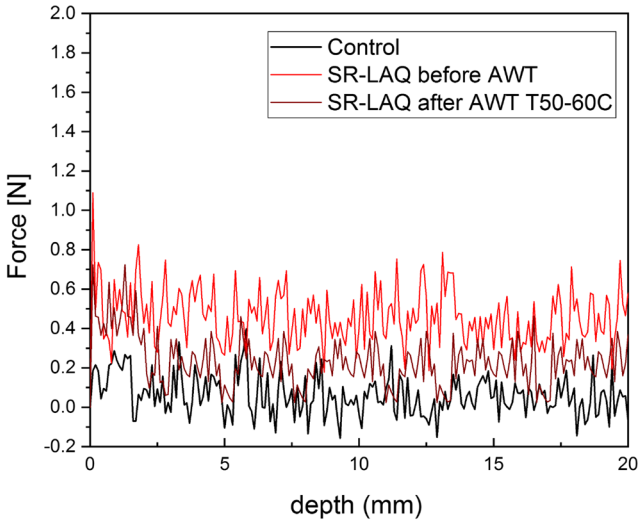
Control
SR-LAQ before AWT
SR-LAQ after AWT T50-60C
Force [N]
depth (mm)

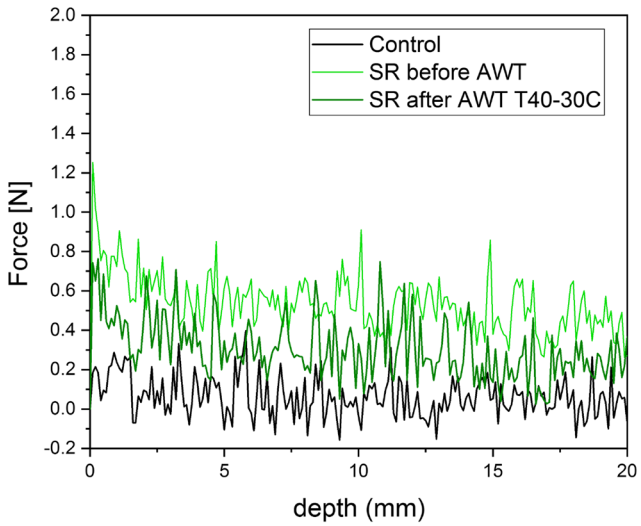
Control
SR before AWT
SR after AWT T40-30C
Force [N]
depth (mm)

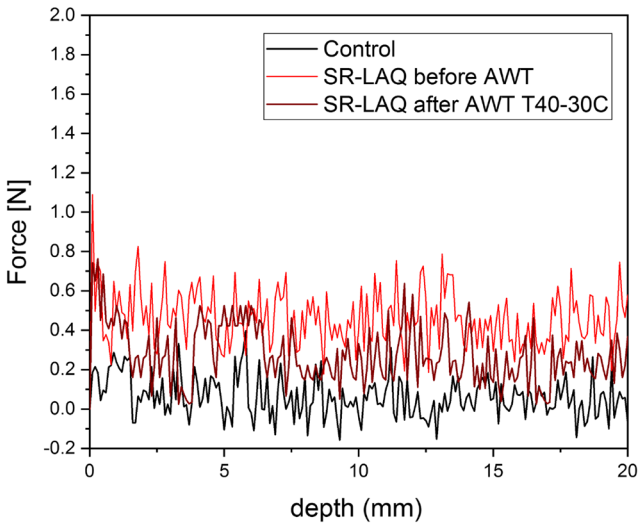
Control
SR-LAQ before AWT
SR-LAQ after AWT T40-30C
Force [N]
depth (mm)

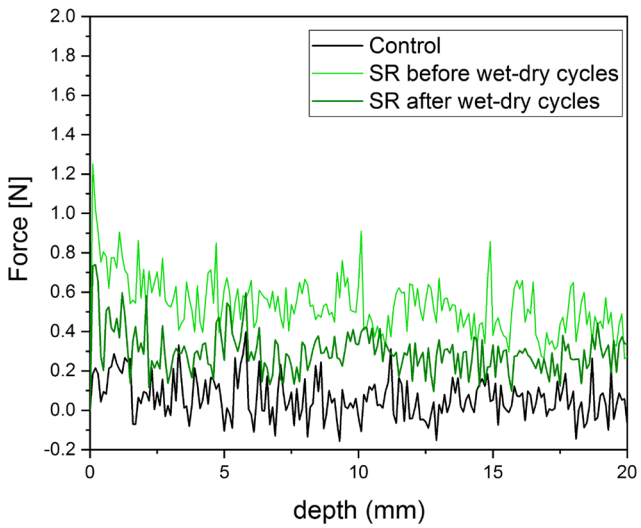
Control
SR before wet-dry cycles
SR after wet-dry cycles
Force [N]
depth (mm)

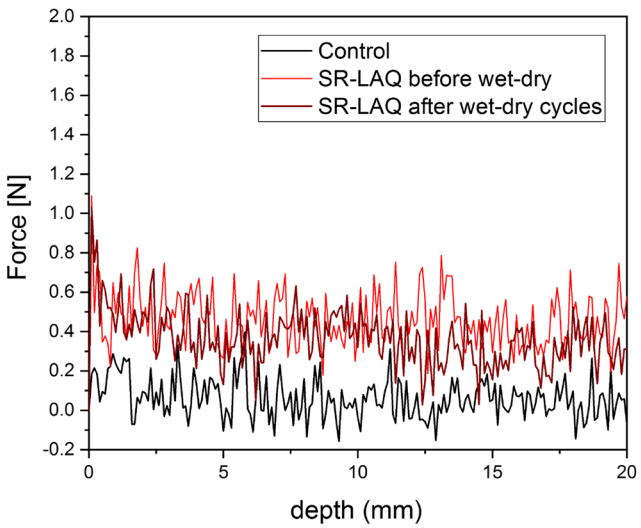
Control
SR-LAQ before wet-dry
SR-LAQ after wet-dry cycles
Force [N]
depth (mm)

applying the nanolime. It was shown that porosity changed with a significant decrease in larger pores (between 2 and 11 μm) and a minor decrease in two ranges of smaller pores (0.01–0.3 μm and 0.5–1 μm). Water absorption results reflected the hydrophobic effect of the samples treated, or pre-treated with SR, while the initial drying rate for all treated specimens was slower than that of the control, no significant difference was observed between the LAQ samples and those treated with SR.

The Scotch Tape Test and the Drilling Resistance measurements showed that pre-treatment with SR resulted in both an increased surface cohesion and penetration depth. Since the amount of nanolime introduced was the same for both LAQ by itself or when applied over the SR, the DRMS patterns suggest that nanolime could be distributed more homogeneously throughout the pores in the sample when applied after a pre-treatment with SR, as in this sample the nanoparticles did not accumulate in the outer 6–8 mm. SEM images show that nanolime particles are completely embedded in the sticky rice film in the pores, where they crystalized. Both DRMS and SEM results support the hypothesis that the sticky rice film could attach nanolime particles to the film during the application of nanolime, reducing the back-migration of the nanoparticles thus contributing to their in-depth deposition and providing a homogenous distribution throughout the sample. This topic needs further study to determine the influence of sticky rice on the penetration of nanolime. Finally, the colorimetric results show that while consolidation with LAQ resulted in a significant whitening effect (ΔE^* 13.87), when pre-treated with sticky rice it was significantly reduced (ΔE^* 8.23), while application of sticky rice by itself was below visual detection level.

Previous studies where the sticky rice was added to lime for mortars reported that between 3 and 5% w/w of SR accelerated the setting and hardening (i.e., increased compressive strength) and bonding capability, although unit weight and water resistance were slightly reduced [16]. Another study [3] showed that consolidated samples could resist a 2 months water immersion without falling apart as the control samples did. This study focused on the effect that sticky rice would have as a consolidant, either by itself or followed by a nanolime consolidation treatment applied to low resistance mortars. This is a significant difference in approach than the traditional Chinese application and therefore previous studies cannot be compared directly. The weathering cycles used in this study to test the resistance of the treated samples showed that they are susceptible to wet–dry cycling damage, particularly if subjected to higher temperature changes since the gelatinization process of the amylopectin occurs at temperatures above 55 °C [50]. During this degradation process, the sticky rice samples acquired a yellowish tinge, which was measured by colorimetric analysis ($\Delta E \sim 3$). Future studies should also consider the reapplication of sticky rice solution after the nanolime consolidation.

SEM images of the treated samples show morphological differences between the two treatments involving sticky rice (SR and SR-LAQ). SR samples show that sticky rice forms a film over the substrate grains, while the SR-LAQ samples show calcite crystals growing up embedded in the sticky rice film. However, the growth of the calcite crystals in the presence of sticky rice was similar to the calcite crystal size reported in previous studies [24] confirming that they did not reduce in size as happens when sticky rice and lime are mixed together during the manufacture of the mortar [4, 15]. In this case, the amylopectin was found to play a crucial role in the carbonation process of $Ca(OH)_2$ inhibiting the growth of the $CaCO_3$ crystals so that only smaller calcite crystals developed forming a dense and compact microstructure that reduces the penetration of water and increases their durability [15, 18]. This is a significant difference that reflects the disparities in approach, the Chinese studies focused on mortar preparation, while this one concentrates on their consolidation.

The presence of the sticky rice may increase biocolonization of the treated area, since it is close to the surface, and needs to be considered. In the traditional method where the sticky rice was added during the lime quenching, bacteria were eliminated by the released heat [7, 10]. In the present situation, where the SR is applied directly to the object biocolonization may develop faster, especially in areas where moisture prevails. However, since wet–dry cycling of the treated object will first eliminate the SR from the surface, the biocolonization may be retarded. This is a point that needs to be taken into account in future research.

Further studies with sticky rice are needed to understand the deterioration process of the sticky rice

and if damage could be caused by the swelling that occurs during starch hydrolysis. Additionally, the long-term biodegradation effect on this polysaccharide needs to be evaluated since it can be a source of nutrients for microorganisms. Although more research is required to evaluate the promising consolidation results obtained, such as actual depth of penetration and repeating the application of sticky rice after the nanolime, it could be preliminary concluded that sticky rice nanolime consolidation could be used to repair weathered materials in very dry environments (e.g., Mediterranean Eastern countries) or in interior spaces where no liquid water is to be found.

Conclusions

The promising results from this innovative research showed that the use of sticky rice alone or in combination with LAQ nanolime yields a higher degree of consolidation than that attained by a simple nanolime consolidation. However, the consolidation effectiveness of sticky rice decreases when the treated samples are exposed to weathering processes. More research needs to be carried out to fully understand the sticky rice weathering process to optimize its consolidation mechanism.

This study has shown that:

- The sticky rice solution has low viscosity which favors good penetration into the porous substrate. FTIR and the iodine test confirm that the sticky rice starch is composed mainly of amylopectin. The morphological properties of the dried gelatinized sticky rice show that it presents an uneven structure formed by a film with several granular nodules tightly packed and clustered into compound grains.
- All treated samples, either with nanolime (LAQ), sticky rice (SR) or their combination (SR-LAQ), had a lower porosity. The highest porosity decrease was observed for samples treated with SR-LAQ (~ 22.9% decrease), followed by those treated with SR (12.8%). MIP results clearly show that the reduction in porosity corresponds to the filling of pores with diameters between 2 and 11 μm in all treatments. Both treated samples involving nanolime, i.e., LAQ and SR-LAQ, also showed a reduction in the smaller pore range with diameter between 0.01 and 0.3 μm and confirming that LAQ can partially fill these finer pores.
- A significant increase of surface cohesion. The samples treated with only sticky rice showed the highest increase in the superficial cohesion followed by samples treated with sticky rice and nanolime.
- A certain degree of hydrophobicity was imparted to the sample surface by the application of the SR, but it decreases when nanolime is applied subsequently. Further studies are required to elucidate this behavior.
- The drilling resistance increases for all treated samples, especially those pre-treated with sticky rice, where the treatment certainly reached 2 cm (half the length of the sample reached by the drilling) while those treated only with LAQ merely reach 6 mm. The increase in the drilling resistance is fairly constant throughout the drilling depth, confirming that sticky rice starch increases the mechanical resistance of samples providing a deeper consolidation of the mortar independent of the use of nanolime in combination with it. The increased durability of the SR-LAQ treatment could be attributed to the sticky rice which apparently improved nanolime distribution throughout the sample. Further research is required to elucidate this hypothesis and to study the total penetration depth of the sticky rice independent of the use of nanolime in combination with it.
- Colorimetric results show that both samples involving nanolime (LAQ and SR-LAQ) caused a slight whitening of the surface with both ΔE^* and ΔL^* values above 5.
- The surface cohesion, hydrophobicity and drilling resistance of sticky rice samples significantly decreased after exposure of the samples to the AWT-1 (T = 40–60 °C) weathering which may be attributed to the irreversible starch gelatinization process.
- A lower decrease in the consolidation was noticeable after exposure of the samples to the AWT-2 (T = 40–30 °C) and similar results were obtained after wet–dry cycles. These results confirm that starch still degrades at medium or room temperatures after several moisture cycles.
- FTIR analysis of the water from wet–dry cycles shows that small amounts of sticky rice starch was dissolved in the water.

- The decrease in surface cohesion, hydrophobicity and drilling resistance after any of the weathering processes tested is more pronounced in SR samples than in SR-LAQ. This could be attributed to the presence of the calcite crystals growing on the sticky rice film which might increase the adhesion to the matrix of both calcite and starch film, as both may bond to the matrix physically and chemically due to the calcite–calcite bonding, reducing the solubilization of the sticky rice film.

Acknowledgements

This research has been funded by the Vice Chancellor's Scholarship within the Doctorate Program by Sheffield Hallam University (UK) and through the Cantor Mobility Scholarship Scheme for my research stay at the Smithsonian Institution (USA).

Electronic supplementary material: The online version of this article (https://doi.org/10.1007/s10853-019-03618-1) contains supplementary material, which is available to authorized users.

Open Access This article is distributed under the terms of the Creative Commons Attribution 4.0 International License (http://creativecommons.org/licenses/by/4.0/), which permits unrestricted use, distribution, and reproduction in any medium, provided you give appropriate credit to the original author(s) and the source, provide a link to the Creative Commons license, and indicate if changes were made.

References

[1] Snow J, Torney C (2014) Lime mortars in traditional buildings. Short guide 6. Historic Scotland, Edinburgh

[2] Mydin MAO (2017) Preliminary studies on the development of lime-based mortar with added egg white. Int J Technol 5:800–810

[3] Zeng Y, Zhang B, Liang X (2008) A case study and mechanism investigation of typical mortars used on ancient architecture in China. Thermochim Acta 473:1–6

[4] Yang T, Ma X, Zhang B, Zhang H (2016) Investigations into the function of sticky rice on the microstructures of hydrated lime putties. Constr Build Mater 102(1):105–112

[5] Gadhave RV, Mahanwar PA, Gadekar PT (2017) Starch-based adhesives for wood/wood composite bonding: review. Open J Polym Chem 7:19–32

[6] Alcazar-Alay SC, Almeida-Meireles MA (2015) Physico-chemical properties, modifications and applications of starches from different botanical sources. Food Sci Technol 35(2):215–236. https://doi.org/10.1590/1678-457X.6749

[7] Wang L, Xie Y, Wu Y, Guo Z, Cai Y, Xu Y, Zhu X (2012) Failure mechanism and conservation of the ancient seawall structure along Hangzhou Bay, China. J Coast Res 28(6):1393–1403

[8] Wei G, Zhang H, Wang H, Fang S, Zhang B, Yang F (2012) An experimental study on application of sticky rice–lime mortar in conservation. Constr Build Mater 28:624–632

[9] Luo YB, Zhang YJ (2013) Investigation of sticky-rice lime mortar of the Horse Stopped Wall in Jiange. Herit Sci 1:26–30

[10] Xiao Y, Fu X, Gu H, Gao F, Liu S (2014) Properties, characterization, and decay of sticky rice–lime mortars from the Wugang Ming Dynasty City Wall (China). Mater Charact 90:164–172

[11] Liu X, Ma X, Zhang B (2016) Analytical Investigations of traditional masonry mortars from Ancient City Walls Built during Ming and Qing Dynasties in China. Int J Archit Herit 10(5):663–673. https://doi.org/10.1080/15583058.2015.1104399

[12] Song Y (1958) Tian Gong Kai Wu. Commercial Press, Shanghai, p 197

[13] Archaeology Crew of Henan Province (1958) A brick tomb with colorized portrait in Deng country. Henan Province, Cultural Relic Press, Beijing, p 20

[14] Song Y, Wu TGK (1982) The exploitation of the works of nature first written in 1587. Times and Culture Publishing Co., Taibei

[15] Yang F, Zhang B, Ma Q (2010) Study of sticky rice—lime mortar technology for the restoration of historical masonry construction. Acc Chem Res 43(6):936–944

[16] Zhao P, Jackson MD, Zhang Y, Li G, Monteiro PJM, Yang L (2015) Material characteristics of ancient chinese lime binder and experimental reproductions with organic admixtures. Constr Build Mater 84:477–488

[17] Yang R, Zhang Z, Xie M, Li K (2016) Microstructural insights into the lime mortars mixed with sticky rice sol-gel or water: a comparative study. Constr Build Mater 125:974–980

[18] Yang R, Li K, Wang L, Bornert M, Zhang Z, Hu T (2016) A micro-experimental insight into the mechanical behaviour of sticky rice slurry-lime mortar subject to wetting–drying cycles. J Mater Sci 51(18):8422–8433. https://doi.org/10.1007/s10853-016-0099-x

[19] Liu Q, Liu Y, Zeng K, Yang F, Hui ZhuH, Liu Q (2011) Advanced design of Chinese traditional materials for the conservation of historic stone buildings. J Archaeol Sci 38:1896–1900

[20] Lin JS, Lin ZJ, Chan JF (2005) The ancient earthquake and earthquake-resistance of ancient building in Quanzhou City. World Earthq Eng 21(2):159–166

[21] Baglioni P, Chelazzi D, Giorgi R, Carretti E, Toccafondi N, Jaidar Y (2014) Commercial $Ca(OH)_2$ nanoparticles for the consolidation of immovable works of art. Appl Phys A 114:723–732

[22] Rodriguez-Navarro C, Ruiz-Agudo E (2017) Nanolime: from synthesis to application. Pure Appl Chem 90(3):523–550. https://doi.org/10.1515/pac-2017-0506

[23] Otero J, Charola AE, Grissom CA, Starinieri V (2017) An overview of nanolime as a consolidation method for calcareous substrates. Ge-conservación 11:71–78

[24] Otero J, Starinieri V, Charola AE (2018) Nanolime for the consolidation of lime mortars: a comparison of three available products. Constr Build Mater 181:394–407

[25] Daniele V, Taglieri G, Quaresima R (2008) The nanolime in cultural heritage conservation: characterization and analysis of the carbonation process. J Cult Herit 9(3):294–301

[26] Lopez-Arce P, Zornoza-Indart A (2015) Carbonation acceleration of calcium hydroxide nanoparticles: induced by yeast fermentation. Appl Phys A 120(4):1475–1495

[27] Borsoi G, Lubelli B, Van Hees RPJ, Rosario-Veiga M, Santos-Silva A (2015) Understanding the transport of nanolime consolidants within Maastricht limestone. J Cult Herit 18:242–249. https://doi.org/10.1016/j.culher.2015.07.014

[28] Borsoi G, Lubelli B, Van Hees R, Rosario-Veiga M, Santos-Silva A, Fedele L, Tomasin P (2016) Effect of solvent on nanolime transport within limestone: how to improve in-depth deposition. Colloids Surf A 497:171–181

[29] Borsoi G, Lubelli B, van Hees R, Rosario-Veiga M, Santos-Silva A (2016) Optimization of nanolime solvent for the consolidation of coarse porous limestone. Appl Phys A 122:846–856. https://doi.org/10.1007/s00339-016-0382-3

[30] BS EN (1999) 1015-2, Methods of test for mortar for masonry–Part 2: determination of flexural and compressive strength of hardened mortar. European Committee for Standardization, Brussels

[31] BS EN (1999) 1015-3, Methods of test for mortar for masonry–Part 3: determination of flexural and compressive strength of hardened mortar. European Committee for Standardization, Brussels

[32] Rietveld HM (1969) A profile refinement method for nuclear and magnetic structures. J Appl Crystallogr 10:65–71

[33] Bish DL, Post JE (1989) Modern powder diffraction. Mineralogical Society of America, Crystal Research & Technology, Washington. ISBN 0-939950-24-3

[34] Taglieri G, Daniele V, Re Del, Volpe R (2015) A new and original method to produce $Ca(OH)_2$ nanoparticles by using an anion exchange resin. Adv Nanoparticles 4:17–24

[35] Taglieri G, Otero J, Daniele V, Gioia G, Macera L, Starinieri V, Charola AE (2018) The biocalcarenite stone of Agrigento (Italy): preliminary investigations of compatible nanolime treatments. J Cult Herit 30:92–99. https://doi.org/10.1016/j.culher.2017.11.003

[36] Miller BF, Root W (1991) Long-term storage of wheat starch paste. Stud Conserv 36(2):85–92

[37] IRUG (Infrared & Raman Users Group) (2018) Data base, rice starch. Getty Conservation Institute, Los Angeles

[38] Rundl RE, Foster JF, Baldwin RR (1944) On the nature of the Starch–Iodine complex. J Am Chem Soc 66:2116–2120

[39] Kornev KG, Neimark AV (2001) Spontaneous penetration of liquids into capillaries and porous membranes revisited. J Colloids Interface Sci 235:101–113

[40] Rodriguez-Navarro C, Bettori I, Ruiz-Agudo E (2016) Kinetics and mechanism of calcium hydroxide conversion into calcium alkoxides: implications in heritage conservation using nanolimes. Langmuir 32(20):5183–5194

[41] EN 13755 (2008) Natural Stone Test Methods—Determination of Water Absorption at Atmospheric Pressure. European Committee for Standardization, Brussels

[42] ASTM C 67-00 (2000) Standard test methods for measuring apparent porosity at atmospheric pressure. ASTM, Pennsylvania

[43] EN 16322 (2013) European Standard, Conservation of Cultural Heritage – Test Methods – Determination of Drying Properties, European Committee for Standardization (CEN)

[44] ASTM D3359-02 (2002) Standard test methods for measuring adhesion by tape test. ASTM International, Pennsylvania

[45] Costa D, Delgado-Rodrigues J (2012) Consolidation of a porous limestone with nano-lime. In: Proceeding of 12th international congress on the deterioration and conservation of stone. Columbia University, New York, October 22–26, pp 9–20. http://iscs.icomos.org/pdf-files/NewYorkConf/costdelg.pdf

[46] Delgado-Rodrigues J, Ferreira-Pinto AP, Nogueira R, Gomes A (2017) Consolidation of lime mortars with ethyl silicate, nanolime and barium hydroxide. Effectiveness assessment with microdrilling data. J Cult Herit 29:1296–2074. https://doi.org/10.1016/j.culher.2017.07.006

[47] Rodriguez-Navarro C, Suzuki A, Ruiz-Agudo E (2013) Alcohol dispersions of calcium hydroxide nanoparticles for stone conservation. Langmuir 29:11457–11470

[48] Pavlovic S, Brandao P (2003) Adsorption of starch, amylose, amylopectin and glucose monomer and their effect the flotation of hematite and quartz. Miner Eng 16:1117–1122

[49] Walsh Z, Janecek ER, Jones M (2015) Natural polymers as alternative consolidants for the preservation of waterlogged archaeological wood. Stud Conserv 62(3):173–183

[50] Charola AE, Vicenzi EP, Grissom CA, Little N (2017) Composition and characteristics of Kasota limestone on the exterior of the national museum of the American Indian building. In: Conservation of the exterior of the national museum of the American Indian building, vol 6, pp 17–26

[51] Belitz H-D, Werner G, Schieberle P (2004) Food chemistry, 3rd edn. Springer, Berlin, pp 318–323. ISBN 3-540-40818-5

[52] Chandroth KS, Tholath EA (2008) Physicochemical rheological and thermal properties of njavara rice (oryza sativa) starch. J Agric Food Chem 56:12105–12113

Publisher's Note Springer Nature remains neutral with regard to jurisdictional claims in published maps and institutional affiliations.